BME011

Numerical Analysis of the Temperature Pattern, Ablation Area and Residual Tail Length in Porous Liver during Microwave Ablation Process

Pornthip Keangin[1,*], Suchai Pongpakpien[2] and Phadungsak Rattanadecho[2]

[1]Department of Mechanical Engineering, Faculty of Engineering, Mahidol University,
25/25 Phutthamonthon 4 Road, Salaya, Nakhon Pathom, 73170, Thailand.
[2]Department of Mechanical Engineering, Faculty of Engineering, Thammasat University (Rangsit Campus),
99 mu 18, Paholyothin Road, Klong Nueng, Klong Luang, Pathumthani, 12120, Thailand.
*Corresponding Author: E-mail: pornthip.kea@mahidol.ac.th, Tel.: +66 2 8892138 Ext. 6401-3, Fax: +66 2 8892138 Ext. 6429

Abstract

Microwave ablation (MWA) is a process that uses the heat from microwave energy to kill cancer tissue without damaging the surrounding tissue. The effectiveness of this treatment is related to the temperature achieved during the process, heating time, microwave power including the equipment that use during the treatment. Slot microwave antennas are the most popular antennas in treatment because of their small dimensions, low cost to manufacture and highly effective. However, slot microwave antennas to cause residual tail of the heating zone patterns inevitably damages surrounding normal tissues. Hence a treatment that fully conforms to the shape of liver tumor is difficult to achieve even with current optimization strategies. Numerical analysis of the temperature pattern, ablation area and residual tail length in porous liver tissue during MWA process via microwave antennas is presented. The effects of heating time, microwave power and number of slot on temperature pattern, ablation area, and residual tail length in porous liver tissue are studied. The transient heat transfer equation and transient momentum equations (Brinkman model extended Darcy model) coupled with the electromagnetic wave propagation equation is solved using the finite element method (FEM). The one-heat transfer equation under local thermal equilibrium (LTE) model is systematically investigated. In order to verify the accuracy of the present model, the numerical results from the present model (porous media model) have been verified with the numerical results of the bioheat model and the experimental results from previous work with the same conditions. The results show that the present model (porous media model) is in agreement with experimental data better than bioheat model. It is found that an increase in the heating time and an increase in the microwave power results in an increase in the maximum temperature, ablation area and residual tail length. However, an increase in the number of slot results in a decrease in the ablation area and increase in the residual tail length. The numerical model in this study can be used as a basis for the development for the practical treatment of liver cancer MWA.

***Keywords**:* Finite element, Liver tissue, Microwave ablation, Porous media, Slot antenna

1. Introduction

Microwave ablation (MWA) is an efficacious treatment for organ cancers, especially liver cancer. MWA can improve outcomes with few side effects for patients and also particularly useful when the cancer cells are located in an area that cannot surgical resection. The main advantages of MWA technology, when compared with existing thermal ablation technologies, include consistently higher internal temperatures, larger ablation areas and faster ablation times [1]. MWA is a process that uses the heat from microwave energy to kill cancer cells [2]. The energy from the microwave is emitted by the microwave antenna to the target tumor/cancer cells. When the microwave energy propagates in a cancer cells, it is absorbed by the medium causes water molecules to vibrate and rotate, resulting in heat to a temperature high enough to cause cancer cell death. The goal of MWA is to elevate the temperature of cancerous tissue cancer to more than 50 °C where cancer cells are destroyed [3] and without the damaging surrounding healthy tissue. The effectiveness of this treatment is related to the temperature achieved during the process, heating time, microwave power including the equipment that use during the treatment.

Microwave antenna is one of the factors that can affect to effectiveness MWA therapy. Several microwave antennas have been developed for MWA within the liver cancer, such as the slot antenna [4-5], floating sleeve antenna [6-7], triaxial antenna [8-9] and cooled-shaft antenna [10-11]. However, the slot antenna is the most popular antennas in treatment because of their small dimensions, low cost to manufacture and highly effective [12]. Moreover, the heating pattern of the slot antenna is uniform and spherical-like heating region, which is more suitable for the most tumor/cancer cells shape [13]. Of many previous studied on heat transfer within liver cancer for interstitial MWA using slot antenna. Keangin et al. [14] carried out on the numerical simulation of liver cancer treated during MWA process using single slot and double slots antennas. The influences of antenna types on microwave power absorbed, specific absorption rate (SAR) and temperature distribution were systematically investigated. However, slot microwave antennas to cause residual tail of the heating zone patterns inevitably damages surrounding normal tissues. This is why a treatment that fully conforms to the shape of liver tumor is difficult to achieve even with current optimization strategies. In recent years, most previous studies of MWA therapy were mainly focused on effects of antenna types on ablation area and did not consider residual tail length caused an incomplete analysis of the results [15-17]. Phasukkit et al. [16] analyzed of triple-antenna configurations and designs for hepatic MWA using 3D finite element method (FEM) and verified by in-vitro experiments. The comparison of coagulation volumes created, as well as temperature distribution characteristics, from the three-antenna arrangements was presented. The results illustrated that arranging antennas in the T-shaped pattern destroyed more unwanted tissues than those found when using linear array and triangular arrangements, with maximum coagulation volume. While clinical treatment with MWA needs to control the temperature distribution and the lesion generation accurately, in order to ensure cancer cells destruction and to minimize side effects to surrounding normal tissue and surrounding other organs [14]. There are few studies on both the ablation area and residual tail length during MWA process in a realistic physical model of the liver cancer in the couple way due to the complexity of the problem, even though it is directly related to thermal injury of tissue. Moreover, in realistic, the biological tissue, such as liver tissue including cell and microvascular bed with the blood flow direction contains many vessels and can be regarded as a porous structure [18-19]. Thus, the study of heat transport in biological tissue should use porous media theory. A few studies considered model of heat transport porous media biomaterials and concentration of layered biomaterials, especially a detailed study of the effects of heating time, input microwave power and number of slot on temperature pattern, ablation area, and residual tail length. This is because complexity of the dielectric and thermal properties in each layer as affected by the temperature pattern, ablation area, and residual tail length within the layered materials. The complete mathematical model is useful for the development of biomedical technologies, especially the actual process of MWA for human liver cancer technology.

In this study, the influences of heating time, microwave power and number of slot on temperature pattern, ablation area, and residual tail length within the porous liver tissue during MWA process have been investigated. The two layers of porous liver tissue model (tumor layer and normal liver tissue layer) are proposed. Mathematical model of the process involved in MWA are based on transient momentum equations (Brinkman model extended Darcy model) and energy equation coupled with electromagnetic wave propagation equation. The coupled nonlinear set of governing equations as well as initial and boundary conditions are solved using the axisymmetric FEM via COMSOL™ Multiphysics. The one-heat transfer equation under local thermal equilibrium (LTE) model is systematically investigated. In order to verify the accuracy of the present model, the numerical results from the present model (porous media model) have been verified with the numerical results of the bioheat model and the experimental results from previous work with the same conditions. The simulation results of temperature pattern, ablation area, and residual tail length are presented in details. This investigation provides the essential aspects for a fundamental understanding of heat transport within liver cancer MWA and can be used as a guideline to evaluate new hypothetical designs.

2. Problem Statement

2.1 Slot microwave antenna model

This study uses a slot microwave antenna, to transfer microwave power into the porous liver for the treatment of liver cancer. The antenna is composed of a thin semi-rigid coaxial cable. Since the antenna is intended to be inserted into the human liver, it is desirable that the outer diameter be as small as possible. This antenna has a diameter of 1.79 mm [14] because the thin antenna is required in the interstitial treatments. A ring-shaped slot, 1 mm wide is cut off the outer conductor 5.5 mm in length from the short circuited tip of the antenna to allow electromagnetic wave propagation into the liver because the effective heating around the tip of the antenna is very important to the interstitial heating and because the electric field becomes stronger near the slot [20]. The width of slot is a 1 mm, which is easily fabricated, and also gives minimal power reflection [5]. The antennas are composed of an inner conductor, a dielectric and an outer conductor. The antennas are enclosed in a catheter (made of polytetrafluorethylene; PTFE), for hygienic to prevent adhesion of the probe to desiccated ablated tissue and guidance purposes. Fig. 1 shows the model geometry of a slot microwave antenna. The antenna is operated at the frequency of 2.45 GHz, a widely used frequency in MWA and is one of the ISM (Industrial, Scientific, and Medical) dedicated frequencies. Dimensions of a slot microwave antenna are given in Table. 1[2]. While the dielectric properties of a slot microwave antenna are given in Table. 2 [2].

2.2 Porous liver model

The porous liver consists of two parts, namely, the tumor and normal liver tissue. The porous liver is considered as a cylindrical geometry, it has a 30 mm radius and 80 mm in height [14]. The tumor is a spherical shape with diameter of 20 mm [2]. The antennas are inserted into the porous liver with 70.5 mm depth [2]. An axially symmetric model is considered in this study, which minimized the computation time while maintaining good resolution and represents the full 3D result. The vertical axis is oriented along the longitudinal axis of the antenna, and the horizontal axis is oriented along the radial direction. Fig. 2 shows the axially symmetrical model geometry for analysis when using a slot microwave antenna.

As mentioned in the section above, in realistic, the biological tissue, such as liver tissue including cell and microvascular bed with the blood flow direction contains many vessels and can be regarded as a porous structure. Three main compartments of porous liver are identified namely, blood vessels, cells and interstitial space [18-19]. The interstitial space can be further divided into the extracellular matrix and the interstitial blood. However, for sake of simplicity, the porous liver are divided into two distinctive regions, namely, the vascular region (blood vessels) and the extra-vascular region (cells and the interstitial space) and treat the whole anatomical structure as a fluid-saturated porous medium, through which the blood infiltrates. The vascular region is regarded as a blood/fluid phase and extra-vascular region is regarded as a tissue/solid phase, as illustrated in Fig. 2.

The thermal and dielectric properties of normal tissue, blood and tumor used for simulation are selected from several literatures [5,21-24] and given in Table. 3 where the microwave frequency of 2.45 GHz is considered.

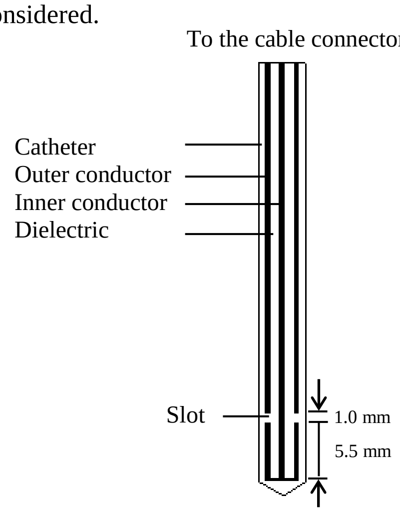

Fig. 1 Model geometry of a slot microwave antenna [2]

Table. 1 Dimensions of a slot microwave antenna

Materials	Dimensions (mm)
Inner conductor	0.135 (radial)
Dielectric	0.335 (radial)
Outer conductor	0.460 (radial)
Catheter	0.895 (radial)
Slot	1.000 (wide)

Table. 2 The dielectric properties of a slot microwave antenna

Properties	Dielectric	Catheter	Slot
Relative permittivity, ε_r (-)	2.03	2.1	1
Electric conductivity, σ (S/m)	0	0	0
Relative permeability, μ_r (-)	1	1	1

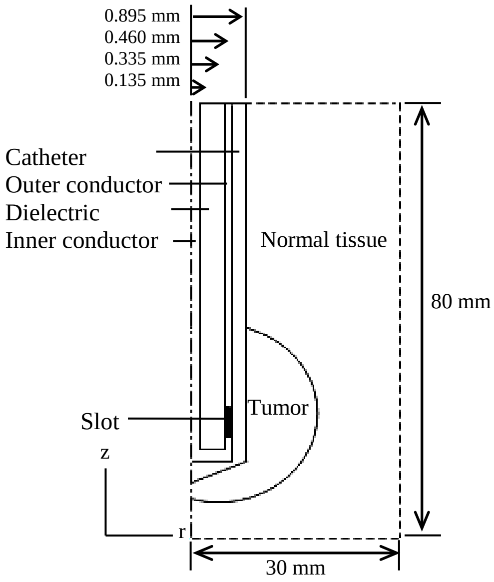

Fig. 2 Axially symmetrical model geometry [2]

3. The formulation of the mathematical model

This study focuses the effects of heating time, microwave power and number of slot on temperature pattern, ablation area and residual tail length in porous liver. An analysis of electromagnetic wave propagation, blood flow and heat transfer in the porous liver during MWA process are illustrated in the next section.

3.1 Analysis of electromagnetic wave propagation

To simplify the problem, the following assumptions are made:

1. Electromagnetic wave propagation is modeled in 2D axially symmetrical cylindrical coordinates (r-z).
2. An electromagnetic wave, propagating in a slot microwave antenna, is characterized by transverse electromagnetic fields (TEM) [5].
3. In the porous liver, an electromagnetic wave is characterized by transverse magnetic fields (TM) [5].
4. The model assumes that the wall of the slot microwave antenna is a perfect electric conductor (PEC).
5. The outer surface of the porous liver is truncated by a scattering boundary condition [14].
6. The model assumes that dielectric properties of the porous liver are uniform and constant.

The electric and magnetic fields associated with the time-varying TEM wave is expressed in 2D axially symmetrical cylindrical coordinates:

Electric field ($\vec{E}$)

$$\vec{E} = e_r \frac{C}{r} e^{j(\omega t - kz)} \tag{1}$$

Magnetic field ($\vec{H}$)

$$\vec{H} = e_\varphi \frac{C}{rZ} e^{j(\omega t - kz)} \tag{2}$$

where $C=\sqrt{\dfrac{ZP}{\pi.\ln\left(r_{outer}/r_{inner}\right)}}$, Z is the wave impedance(Ω), P is the microwave power (W), r_{inner} is the dielectric inner radius (m), r_{outer} is the dielectric outer radius (m), $\omega=2\pi f$ is the angular frequency (rad/s), f is the frequency (Hz), $k=\dfrac{2\pi}{\lambda}$ is the propagation constant (m^{-1}) and λ is the wave length (m).

In the porous liver, the electric field also has a finite axial component, whereas the magnetic field is purely in the azimuth direction. The electric field is in the radial direction only inside the coaxial cable and in both radial and the axial direction inside the tissue. This allows for the slot microwave antenna to be modeled using an axisymmetric TM wave formulation. The wave equation then becomes scalar in $\vec{H}_\varphi$ [14]:

$$\nabla\times\left(\left(\varepsilon_r-\frac{j\sigma}{\omega\varepsilon_0}\right)^{-1}\nabla\times\vec{H}_\varphi\right)-\mu_r k_0{}^2\vec{H}_\varphi=0 \quad (3)$$

where $\varepsilon_0=8.8542\times10^{-12}$ F/m is the permittivity of free space, ε_r is the relative permittivity (-), σ is the electric conductivity (S/m), μ_r is the relative permeability (-) and k_0 is the free space wave number (m^{-1}).

Boundary condition for electromagnetic wave propagation analysis

At the inlet of the slot microwave antenna, TM wave propagation with various microwave powers is considered. An axial symmetry boundary is applied at $r=0$:

$$\vec{E}_r=0 \quad (4)$$

$$\frac{\partial\vec{E}_z}{\partial r}=0 \quad (5)$$

The scattering boundary conditions for $\vec{H}_\varphi$ were used along the outer sides of the porous liver boundaries to prevent reflection artifacts:

$$\hat{n}\times\sqrt{\varepsilon}\vec{E}\text{-}\sqrt{\mu}\vec{H}_\varphi=-2\sqrt{\mu}\vec{H}_{\varphi0} \quad (6)$$

where $\vec{H}_{\varphi0}=C/Zr$ is the excitation magnetic field.

The inner and outer conductors of the slot microwave antenna are modeled as the PEC boundary conditions:

$$\hat{n}\times\vec{E}=0 \quad (7)$$

3.2 Analysis of blood flow and heat transfer

The surroundings of the porous liver model are fixed temperature at 37 °C (normal body temperature) except at the outer surface between the slot microwave antenna and the porous liver is considered as adiabatic boundary condition. To reduce complexity of the problem, several assumptions have been offered into the blood flow and energy equations:

1. Corresponding to electromagnetic wave propagation analysis, blood flow and heat transfer analysis in the porous liver is assumed in 2D axially symmetrical cylindrical coordinates (r-z).
2. The porous liver is assumed to be homogeneous and thermally isotropic and saturated with a fluid (blood).
3. There is local thermodynamic equilibrium (LTE) between blood/fluid phase and tissue/solid phase [2].
4. There is no phase change occurs within the porous liver, no energy exchange through the outer surface of the porous liver, and no chemical reactions occur within the porous liver.
5. The thermal properties of the porous liver are assumed to be constant.

3.2.1 Momentum Equations. The Brinkman model extended Darcy model are used for describing the heat transfer phenomenon [2]:

Continuity equation:

$$\frac{\partial u}{\partial r}+\frac{\partial w}{\partial z}=0 \quad (8)$$

Momentum equations:

$$\frac{1}{\phi}\left(\frac{\partial u}{\partial t}\right)+\frac{1}{\phi^2}\left(u\frac{\partial u}{\partial r}+w\frac{\partial u}{\partial z}\right)=-\frac{1}{\rho_b}\left(\frac{\partial p}{\partial r}\right)+\frac{\nu}{\phi}\left(\frac{\partial^2 u}{\partial r^2}+\frac{\partial^2 u}{\partial z^2}\right)-\frac{u\nu}{\kappa} \quad (9a)$$

$$\frac{1}{\phi}\left(\frac{\partial w}{\partial t}\right)+\frac{1}{\phi^2}\left(u\frac{\partial w}{\partial r}+w\frac{\partial w}{\partial z}\right)=-\frac{1}{\rho_b}\left(\frac{\partial p}{\partial z}\right)+\frac{\nu}{\phi}\left(\frac{\partial^2 w}{\partial r^2}+\frac{\partial^2 w}{\partial z^2}\right)-\frac{w\nu}{\kappa}+g\beta\left(T-T_\infty\right) \quad (9b)$$

where u and w are the blood velocity component in r and z axial, respectively (m/s), ϕ is the porosity, which in this study used ϕ_n = 0.6 and ϕ_t = 0.7 [2], p is the pressure (Pa), ν = 3.78x10^{-7} m^2/s is the kinematics viscosity, β = 1×10^{-4} 1/K is the coefficient of the thermal expansion and κ is the permeability (m^2) can be expressed by the following [25-26]:

$$\kappa=\frac{\phi^3 d_p^2}{175\left(1-\phi\right)^2} \quad (10)$$

where d_p = 1x10^{-4} m^2 is the diameter of cell tissue.

3.2.2 Energy Equation. The transient energy equation based on LTE assumption can be written as [2]:

$$\left(\rho C_p\right)_{eff}\frac{\partial T}{\partial t}+\left(\rho C_p\right)_b\left(u\frac{\partial T}{\partial r}+w\frac{\partial T}{\partial z}\right)= K_{eff}\left(\frac{\partial^2 T}{\partial r^2}+\frac{\partial^2 T}{\partial z^2}\right)+Q_{met}+Q_{ext} \quad (11)$$

where $\left(\rho C_p\right)_{eff}=(1-\phi)\left(\rho C_p\right)_t+\phi\left(\rho C_p\right)_b$ (12)

$$K_{eff}=(1-\phi)K_t+\phi K_b \quad (13)$$

are the overall heat capacity per unit volume and overall thermal conductivity, subscripts eff , t and b represent the effective value, tissue/solid phase and blood/fluid phase, respectively, T is the temperature (°C), ρ is the density (kg/m^3), C_p is the specific heat capacity (J/kg.°C) and K is the thermal conductivity of the liver (W/m·°C).

The Q_{met} = 33,800 W/m^3 is the metabolic heat source term and Q_{ext} is the external heat source (heat generation by the electric field) term, respectively. The external heat source term is equal to the resistive heat generated by the electromagnetic field and assume only generated from tissue phase which can be defined as [27]:

$$Q_{ext}=\frac{\sigma\left|\bar{E}\right|^2}{2} \quad (14)$$

Boundary condition for blood flow and heat transfer analysis

The blood flow and heat transfer analysis are considered only in the porous liver, which does not include the slot microwave antenna. The boundary condition for blood flow and heat transfer analysis as follows:

An axial symmetry boundary is applied at $r=0$ for the blood flow and heat transfer analysis:

$$\hat{n}.\bar{u}=0 \quad (15)$$

$$\hat{n}.\left(-pI+(1/\phi)\eta\left(\nabla.\bar{u}+(\nabla.\bar{u})^T\right)\right)=0 \quad (16)$$

$$\hat{n}.\left(K_{eff}\nabla T-\left(\rho C_p\right)_b\bar{u}T\right)=0 \quad (17)$$

The surroundings of the porous liver are fixed temperature at 37°C and the boundaries for blood flow analysis are considered an open boundary condition:

$$\hat{n}.\left(-pI+(1/\phi)\eta\left(\nabla.\bar{u}+(\nabla.\bar{u})^T\right)\right)=-F_0.\hat{n} \quad (18)$$

where η is the dynamic viscosity (Pa.s) and F_0 is the normal stress (N/m^2)

At the outer surface between the slot microwave antenna and the porous liver is considered as adiabatic boundary condition:

$$\hat{n}.\left(K_{eff}\nabla T\right)=0 \quad (19)$$

Furthermore, it is assumed that no contact resistant occurs between the normal tissue and the tumor. Therefore, the internal boundary is assumed to be a continuous:

$$\hat{n}.\begin{pmatrix}-p_t I+\eta_t\left(\nabla.\bar{u}_t+\left(\nabla.\bar{u}_t\right)^T\right)\\ +p_n I-\eta_n\left(\nabla.\bar{u}_n+\left(\nabla.\bar{u}_n\right)^T\right)\end{pmatrix}=0 \quad (20)$$

$$\hat{n}.\begin{pmatrix}K_{eff}\nabla T_t-\left(\rho C_p\right)_b\bar{u}T_t\\ -K_{eff}\nabla T_n-\left(\rho C_p\right)_b\bar{u}T_n\end{pmatrix}=0 \quad (21)$$

The initial temperature of the porous liver is assumed to be uniform at 37 °C and initial condition for the blood velocity and pressure are $u(t_0)=0$ m/s, $w(t_0)=$ 0 m/s and $p(t_0)=0$ Pa

4. Calculation procedure

In this study, the FEM is used to analyze the transient problems. The coupled model of electromagnetic wave propagation, blood flow and heat transfer analysis is solved to demonstrate the temperature pattern, ablation area and residual tail length that occur within the porous liver during MWA. The computational scheme starts with computing an external heat source term by running an electromagnetic wave propagation calculation and subsequently solves the time dependent temperature in the porous liver. All the steps are repeated until the required heating time is reached. The electromagnetic wave propagation equation coupled with the blood flow and energy equations by Eq. (14). The axisymmetric FEM model is discretized using triangular elements with the Lagrange quadratic shape functions. The set of partial differential equations along with their related boundary conditions are coupled and are solved numerically by the FEM using COMSOL™ multiphysics. In order to obtain a good approximation, a fine mesh is specified in the sensitive areas (the vicinity of the tip of the slot microwave antenna, where the temperature is more concentrated). The number of elements where solution is independent of mesh density is found to be around 20,471. It is reasonable to confirm that, at this number of element, the accuracy of the simulation results is independent from the number of elements through the calculation process.

5. Results and Discussion

5.1 Verification of the model

It must be noted in advance that it is very difficult to make direct comparison of the present model results and the experimental results because it is not possible to directly measure the temperature in the porous liver, especially during MWA process. To verify the accuracy of the present model, the resulting data of the porous media model proposed in this study is validated against the numerical results of bioheat model obtained at the same testing condition by Keangin et al. [14]. Moreover, the numerical results from this study are then compared with the experimental results obtained by Yang et al. [23]. Fig. 3 shows the geometry of the validation model obtained by Yang et al. [23]. In the validation model, the microwave power of 75 W with frequency of 2.45 GHz and the initial liver tissue temperature of 8 °C are selected. The slot microwave antenna with a radius of 1.25 mm is inserted into liver tissues 20 mm in depth. The axially symmetrical model is used to analyze the MWA process with the heating time of 50 s. The validation results of the selected test case are illustrated in Fig. 4 for temperature distribution in the liver tissue, with respect to the heating time of 50 s with the positions of 4.5 mm and 9.5 mm away from the slot microwave antenna. It is observed that the all cases temperatures of the liver tissue are increased with increasing time. From the figures, it is found that the simulation results of the porous media model is in agreement with experimental data better than bioheat model over the same approximate time range at both positions, especially at the end stage. This is due to the fact that the porous media model is based on convective heat mode coupled with conduction heat mode. While the bioheat model is manly heat transfer governed by conduction heat mode. Table. 4 shows the comparisons of the root mean square error (RMSE) of the liver tissue temperature between the present study (porous media model) and our previous work [14] (bioheat model) with experiment from Yang et al. [23]. Data from Table. 5 shows that the bioheat model gives greater error than the simulation results obtained from porous media model. Moreover, at the position of 9.5 mm away from the slot microwave antenna, the temperature distribution matches the experimental results better than the temperature distribution at the position of 4.5 mm. Therefore, the developed model based on porous media approach is reasonable and can be used effectively for this problem. This is important to obtain the approaching realistic tissues modeling during MWA.

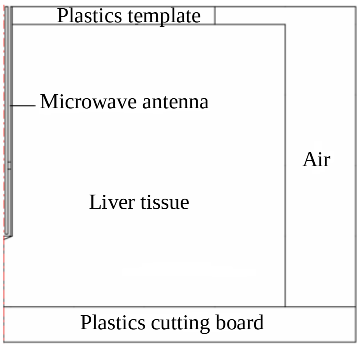

Fig. 3 Geometry of the validation model obtained by Yang et al. [23]

In this study, the influences of the heating time (t), microwave power (P) and number of slot (N) on temperature pattern, ablation area and residual tail length in porous liver tissue have been investigated. The tumor target is a spherical shape with diameter of 20 mm and operating microwave frequency of 2.45 GHz. A parametric study has been carried out to assess the effect of each of these factors separately.

5.2 The effects of heating time

In this topic, the effects of heating time are studied. The heating times of 150 s, 210 s and 300 s are selected for investigation. The physical data are: P = 10 W and N = 1. Figs. 5(a)-5(c) show that the temperature pattern within the porous liver for various heating times of 150 s, 210 s and 300 s, respectively. The figure illustrates the volume heating effect expected from MWA. Microwaves power emitted from the slot microwave antenna propagates through the tumor and the normal tissue, which leads to the generation of a hot spot zone. It is observed that the temperature pattern in all heating times exhibits a near ellipsoidal shape around the slot. It has the highest value in the vicinity of the slot microwave antenna and decreases with the distance lead to the temperature value within the tumor is higher than the temperature value within the normal tissue. This is because the thermal and dielectric property values of tumor are much more than the ones of the normal tissue, as shown in Table. 3. Moreover, it is found that an increase in the heating time results in an increase in the temperature distribution in porous liver.

The ablation area and residual tail length results for various heating times of 150 s, 210 s and 300 are illustrated in Fig. 6(a)-6(c), respectively. The goal of MWA is to elevate the temperature of cancerous tissue cancer to more than 50 °C where cancer cells are destroyed. Therefore, the isothermal contour at 50 °C is considered. It is obvious that increasing the heating time results in an increase in the ablation area in porous liver. However, at the same time residual tail length will also increase. This increasing of residual tail length will effect to surrounding normal tissues. In addition, using long heating time for treatment, result in patients will feel uncomfortable. Comparison of the maximum temperature value, ablation radius, ablation area, ablation volume, ratio between ablation area/ablation zone target and residual tail length for heating times are shown in Table. 5.

5.3 The effects of microwave power

The changing of the microwave powers has significant effects on the temperature pattern, ablation area and residual tail length. The microwave powers of 8 W, 10 W and 12 W are selected for study and demonstration. These microwave powers are selected during MWA in order to estimate the appropriate power setting of MWA applied treatment for liver cancer. The physical data are: N = 1 and t = 300 s. Figs. 7(a)-7(c) show that the temperature pattern within the porous liver for various microwave powers of 8 W, 10 W and 12 W, respectively. It is seen that the temperature pattern in all microwave powers forms a nearly ellipsoidal shape around the slot and the highest value occurs in the vicinity of the slot microwave antenna and decreases with the distance lead to the temperature value within the tumor is higher than the temperature value within the normal tissue corresponds to the effects of heating time. Once again, it can be seen in Fig. 7, an increase in the microwave powers results in an increase in the temperature distribution in porous liver. This is because an increase in the microwave powers results in a higher heat generation rate and lead to temperature increase in porous liver.

Fig. 8(a)-8(c) depict the ablation area and residual tail length results for microwave powers of 8 W, 10 W and 12 W, respectively. Again it can be observed that an increase in the microwave power results in in an increase in the ablation area in porous liver. Nevertheless, at the same time residual tail length will also increase. Likewise, comparison of the maximum temperature value, ablation radius, ablation area, ablation volume, ratio between ablation area/ablation zone target and residual tail length for microwave powers are shown in Table 5. From this table, it can be observed that at microwave power of 12 W has ablation radius, ablation area, ablation volume, ratio between ablation area/ablation zone target higher than at microwave power of 10 W, however, at microwave power of 12 W has residual tail length higher than at microwave power of 10 W of 0.006 m.

5.4 The effects of number of slot

Microwave antenna is one of the factors that can affect to effectiveness MWA therapy. In this section present the effects of number of slot. The comparison of the results from using 1 slot, 2 slots and 3 slots are considered. The slot spacing length of 3.2 mm is selected. The slot spacing length is chosen to achieve localized power deposition near the distal tip of the antenna [2]. The temperature patterns within the porous liver for various numbers of slots of 1 slot, 2 slots and 3 slots are shown in Figs. 9(a)-9(c), respectively. The physical data are: P = 10 W and t = 300 s. It is found that the hot spot zone in all cases forms a nearly ellipsoidal shape around the each slot and the highest value occurs in the vicinity of the each slot microwave antenna and decreases with the distance. In cases of 2 and 3 slots, the slot microwave antenna provides the two hot spot zones with a wider region of temperature pattern to the porous liver around the slot. This is because of in cases 2 and 3 slots have supplied microwave energy via its slot separately. It concludes that the 1 slots microwave antenna is generally suitable for the narrow tumor size and single tumor. While, the 2 and 3 slots microwave antenna are suitable for the larger tumor size and adjacent tumors.

The ablation area and residual tail length results for numbers of slots of slots of 1 slot, 2 slots and 3 slots are illustrated in Fig. 10(a)-10(c), respectively. However, it is evident from the results that the increasing the number of slot results in a decrease in the ablation area in porous liver. Moreover, at the same time residual tail length will also increase. Comparison of the maximum temperature value, ablation radius, ablation area, ablation volume, ratio between ablation area/ablation zone target and residual tail length for number of slots are shown in Table. 5.

6. Conclusions

This study presents a numerical analysis of the effects of heating time, microwave power and number of slot of microwave antenna on the temperature pattern, ablation area and residual rail length in the two layers porous liver during MWA process. Furthermore, the comparisons of temperature distribution form the present model (porous media model) have been verified with the numerical results of the bioheat model and the experimental results from previous work. The results show that the present model (porous media model) is in agreement with experimental data better than bioheat model. Clinical treatment with MWA needs an accurate control of the lesion generation in order to ensure cancer tissue destruction and to minimize damage to normal tissue. The obtained results represent the accurate phenomena to determine the temperature pattern, ablation area and residual rail length in the porous liver during MWA process. It is found that an increase in the heating time and an increase in the microwave power results in an increase in the ablation area and residual tail length. An increase in the number of slot results in a decrease in the ablation area and also increase in the residual tail length. Although still unable to find the optimum of all parameters, the main idea of effect in each parameter in this work can be propose the completed model, i.e., multi-layered porous media model in order to completely explain the actual process of MWA within the porous liver.

7. Acknowledgement

The authors gratefully acknowledge the financial support for this work provided by the Thailand Research Fund (TRF) and Mahidol University.

8. References

[1] Simon, C.J., Dupuy D.E. and Mayo-Smith, W.W. (2005). Microwave ablation: principles and applications,*Radiographics*, vol. 25, October 2005, pp. S69 – S83.

[2] Rattanadecho, P. and Keangin, P. (2013). Numerical study of heat transfer and blood flow in two-layered porous liver tissue during microwave ablation process using single and double slot antenna, *International Journal of Heat and Mass Transfer*, vol. 58(1-2), March 2013, pp. 457 – 470.

[3] McGahan, J.P., Brock, J.M., Tesluk, H., Gu, W.Z., Schneider, P. and Browing, P.D. (1992). Hepatic ablation with use of radio-frequency electrocautery in the animal model, *Journal of Vascular and Interventional Radiology*, vol. 3(2), May 1992, pp. 291 – 297.

[4] Saito, K., Yoshimura, H., Ito, K., Aoyagi, Y. and Horita, H. (2004). Clinical trials of interstitial

microwave hyperthermia by use of coaxial-slot antenna with two slots, *IEEE Transactions on Microwave Theory and Techniques*, vol. 52(8), August 2004, pp.1987 – 1991.
[5] Bertram, J.M., Yang, D., Converse, M.C., Webster, J.G. and Mahvi, D.M. (2006). Antenna design for microwave hepatic ablation using an axisymmetric electromagnetic model, *Biomedical Engineering* Online, vol. 5, February 2006, pp. 1 – 9.
[6] Yang, D., Bertram, J.M., Converse, M.C., O'Rourke, A.P., Webster, J.G., Hagness, S.C., Will, J.A. and Mahvi, D.M. (2006). A floating sleeve antenna yields localized hepatic microwave ablation, *IEEE Transactions* on *Biomedical Engineering*, vol. 53 (3), March 2006, pp. 533 – 537.
[7] Prakash, P., Deng , G., Converse , M.C., Webster, J.G., Mahvi, D.M. and Ferris, M.C. (2008). Design optimization of a robust sleeve antenna for hepatic microwave ablation, *Physics in Medicine and Biology*, vol. 53(4), February (2008), pp. 1057 – 1069.
[8] Brace, C.L., Van Der Weide, D.W., Lee Jr., F.T., Laeseke, P.F. and Sampson, L. (2004). Analysis and experimental validation of a triaxial antenna for microwave tumor ablation, *IEEE MTT-S International Microwave Symposium Digest*, vol. 3(6-11), January 2004, pp. 1437 – 1440.
[9] Brace, C.L., Laeseke, P.F., Sampson, L.A., Frey, T.M., Van Der Weide, D.W., Lee Jr., F.T. (2007). Microwave ablation with multiple simultaneously powered small-gauge triaxial antennas: results from an in vivo swine liver model, *Radiology*, vol. 244 (1), July 2007, pp. 151 – 156.
[10] Jiao, D., Qian, L., Zhang, Y., Zhang, F., Li, C., Huang, Z., Zhang, L., Zhang, W., Wu, P., Han, X., Duan, G. and Han, J. (2010), Microwave ablation treatment of liver cancer with 2,450-MHz cooled-shaft antenna: an experimental and clinical study, *Journal of Cancer Research and Clinical Oncology*, vol. 136(10), October 2010, pp. 1507 – 1516.
[11] Sun, Y., Cheng, Z., Dong, L., Zhang, G., Wang, Y. and Liang, P. (2012). Comparison of temperature curve and ablation zone between 915- and 2450-MHz cooled shaft microwave antenna: results in ex vivo porcine livers, *European Journal of Radiology*, vol. 81 (3), March 2012, pp. 553 – 557.
[12] Hadizafar, L., Azarmanesh, M.N., and Ojaroudi, M. (2011). Enhanced bandwidth double-fed microstrip slot antenna with a pair of L-shaped slots, *Progress in Electromagnetics Research*, vol. 18, November 2010, pp. 47 – 57.
[13] Drewitz, M., Helbling, M., Fried, N., Bieri, M., Moritz, W., Lichtenberg, J. and Kelm, J.M. (2011). Towards automated production and drug sensitivity testing using scaffold-free spherical tumor microtissues, *Biotechnology Journal Special Issue: Scaffold-free cell-based systems*, vol. 6(12), December 2011, pp. 1488 – 1496.
[14] Keangin, P., Rattanadecho, P. and Wessapan, T. (2011). An analysis of heat transfer in liver tissue during microwave ablation using single and double slot antenna, *International Communications in Heat and Mass Transfer*, vol. 38(6), July 2011, pp. 757 – 766.
[15] Clark ,P.E., Woodruff, R.D., Zagoria, R.J. and Hall, M.C. (2007). Microwave ablation of renal parenchymal tumors before nephrectomy: phase I study, *American Journal of Roentgenology*, vol. 188(5), May 2007, pp. 1212 – 1214.
[16] Phasukkit, P., Tungjitkusolmun, S. and Sangworasil, M. (2009). Finite-element analysis and in vitro experiments of placement configurations using triple antennas in microwave hepatic ablation, *IEEE Transactions on Biomedical Engineering*, vol. 56(11), November 2009, pp. 2564 – 2572.
[17] Li, M., Yu, X.L., Liang, P., Liu, F., Dong, B. and Zhou, P. (2012). Percutaneous microwave ablation for liver cancer adjacent to the diaphragm, *International Journal of Hyperthermia*, vol. 28(3), pp. 218 – 226.
[18] Nakayama, A. and Kuwahara, F. (2008). A general bioheat transfer model based on the theory of porous media, *International Journal of Heat and Mass Transfer*, vol. 51(11-12), June 2008, pp. 3190 – 3199.
[19] Mahjoob, S. and Vafai, K. (2009). Analytical characterization of heat transport through biological media incorporating hyperthermia treatment, *International Journal of Heat and Mass Transfer*, vol. 52(5-6), February 2009, pp. 1608 – 1618.
[20] Saito, K., Hayashi,Y., Yoshimura, H. and Ito,K. (2000). Heating characteristics of array applicator composed of two coaxial-slot antennas for microwave coagulation therapy, *IEEE Transactions on Microwave Theory and Techniques*, vol. 48(11) (1 PART 1), November 2000, pp. 1800 – 1806.
[21] Chen, Z.P., Miller, W.H., Roemer, R.B. and Cetas, T.C. (1990). Errors between two and three dimensional thermal model predictions of hyperthermia treatments, *International Journal of Hyperthermia*, vol. 6(1), January 1990, pp. 175 – 191.
[22] Stauffer, P.R., Rossetto, F., Prakash, M., Neuman, D.G. and Lee, T. (2003). Phantom and animal tissues for modeling the electrical properties of human liver, *International Journal of Hyperthermia*, vol. 19(1), January- February 2003, pp. 89 – 101.
[23] Yang, D., Converse, M., Mahvi, D.M. and Webster, J.G. (2007). Expanding the bioheat equation to include tissue internal water evaporation during heating, *IEEE Transactions on Biomedical Engineering*, vol.54(8), August 2007, pp. 1382 – 1388.
[24] Wessapan, T., Srisawatdhisukul, S. and Rattanadecho, P. (2011). The effects of dielectric shield on specific absorption rate and heat transfer in the human body exposed to leakage microwave energy, *International Communications in Heat and Mass Transfer*, vol. 38(2), February 2011, pp. 255 – 262.
[25] Vafai, K. (1984). Convective flow and heat transfer in variable-porosity media, *Journal of Fluid Mechanics*, vol.147, October 1984, pp 233 – 259
[26] Nield, D.A. and Bejan, A. (1999). Convection in porous media, 2nd ed., Springer-Verlag, Inc., New York.

Table. 3 The thermal and dielectric properties of normal tissue, blood and tumor used for simulation [5,21-24]

Properties	**Thermal conductivity** K (W/m °C)	**Density** ρ (kg/m^3)	**Specific heat capacity** C_p (J/ kg. °C)	**Relative permittivity** ε_r	**Electric conductivity** σ (S/m)
Normal tissue (n)	0.497	1,030	3,600	43.00	1.69
Blood (b)	0.45	1,058	3,960	58.30	2.54
Tumor (t)	0.57	1,040	3,960	48.16	2.096

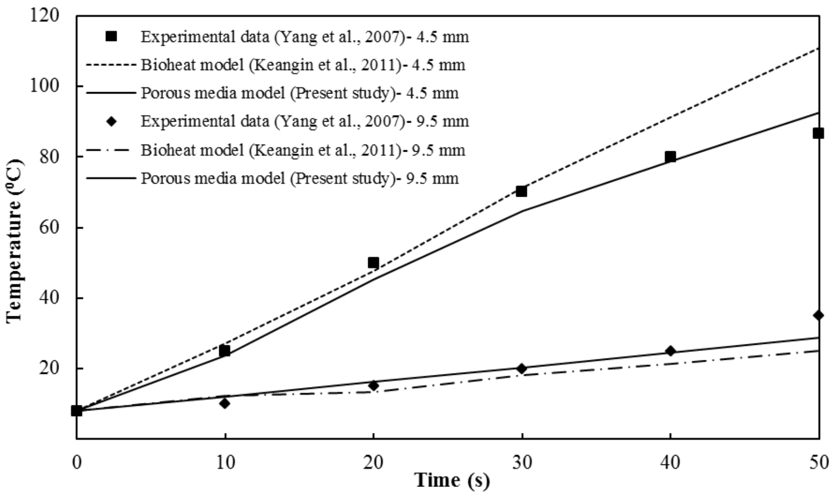

Fig. 4 The validation results of the liver tissue temperature, against Keangin et al. [14] and Yang et al. [23]

Table. 4 Comparisons of RMSE of the liver tissue temperature between the present study and Keangin et al. [14] and Yang et al. [23]

Position (mm)	**Comparisons of RMSE with experiment from Yang et al. [23] (°C)**	
	Bioheat model (Keangin et al. [14])	**Porous media model (Present study)**
4.5 mm	11.10	3.87
9.5 mm	4.52	2.73

Table. 5 Comparison of the maximum temperature value, ablation radius, ablation area, ablation volume, ratio between ablation area/ablation zone target and residual tail length for all cases

	Maximum temperature (°C)	**Ablation radius (m)**	**Ablation area (m^2)**	**Ablation volume (m^3)**	**Ratio (Ablation area / Ablation zone target) (-)**	**Residual Tail Length (m)**
The effects of heating time						
- P = 10 W,N = 1, t = 150 s	76.349	0.0053	0.883x10^{-4}	0.624x10^{-6}	0.2809	0.0284
- P = 10 W,N = 1, t = 210 s	80.242	0.0071	1.582x10^{-4}	1.500x10^{-6}	0.5041	0.0360
- P = 10 W,N = 1, t = 300 s	84.347	0.0081	2.062x10^{-4}	2.227x10^{-6}	0.6561	0.0445
The effects of microwave power						
- P = 8 W,N = 1, t = 300 s	75.510	0.0074	1.721x10^{-4}	1.698x10^{-6}	0.5476	0.0367
- P = 10 W,N = 1, t = 300 s	84.347	0.0081	2.062x10^{-4}	2.227x10^{-6}	0.6561	0.0445
- P = 12 W,N = 1, t = 300 s	93.088	0.0090	2.546x10^{-4}	3.055x10^{-6}	0.8100	0.0504
The effects of number of slot						
- P = 10 W,N = 1, t = 300 s	84.347	0.0081	2.062x10^{-4}	2.227x10^{-6}	0.6561	0.0445
- P = 10 W,N = 2, t = 300 s	82.483	0.0062	1.208x10^{-4}	0.999x10^{-6}	0.3844	0.0543
- P = 10 W,N = 3, t = 300 s	81.035	0.0059	1.094x10^{-4}	0.861x10^{-6}	0.3481	0.0595

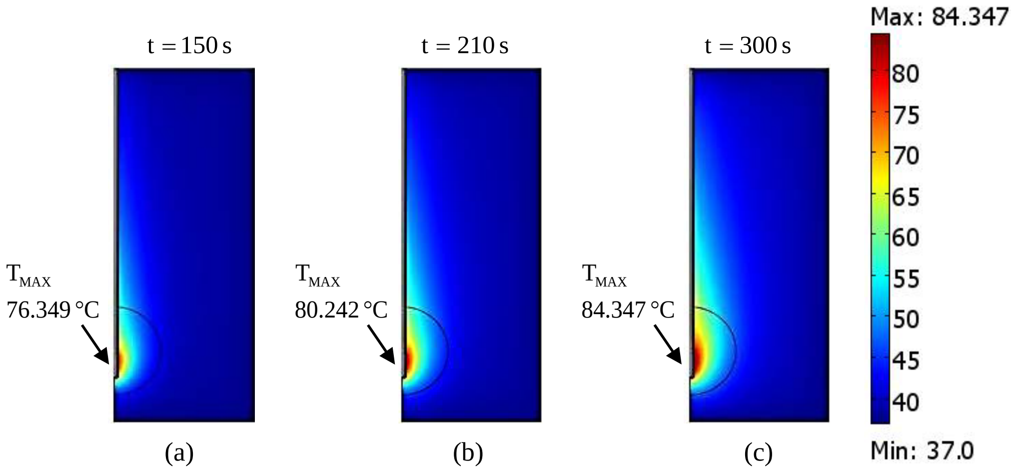

Fig. 5 The temperature pattern within the porous liver base on P = 10 W and N = 1 at various heating times; (a) 150 s (b) 210 s and (c) 300 s

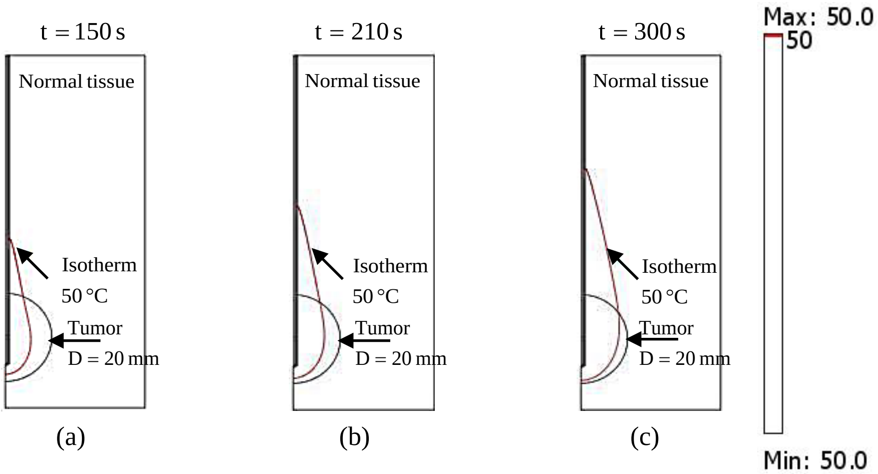

Fig. 6 The ablation area and residual tail length results within the porous liver base on P = 10 W and N = 1 at various heating times; (a) 150 s (b) 210 s and (c) 300 s

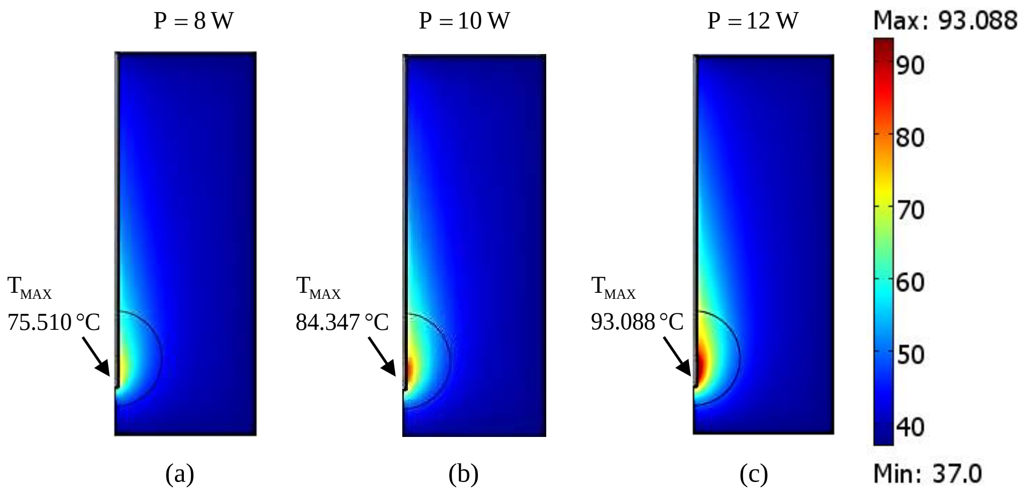

Fig. 7 The temperature pattern within the porous liver base on N = 1 and t = 300 s at various microwave power; (a) 8 W (b) 10 W and (c) 12 W

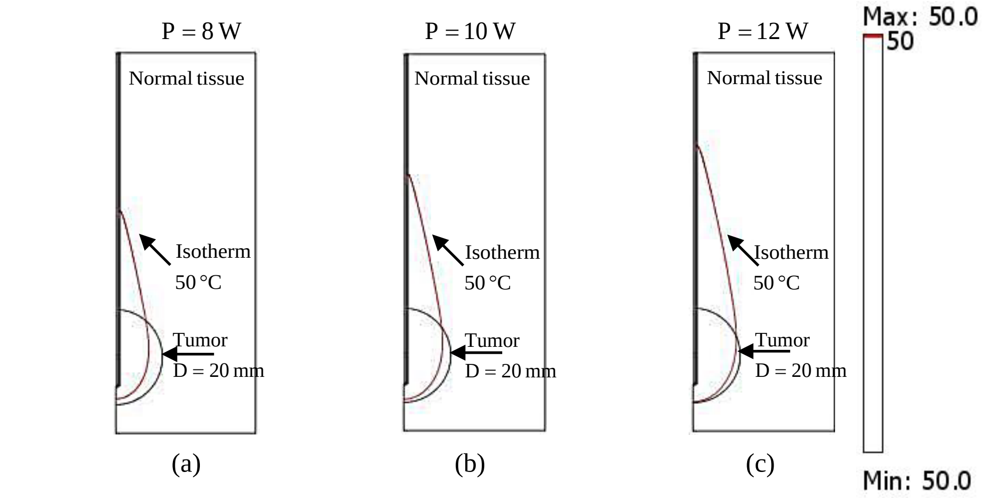

Fig. 8 The ablation area and residual tail length results within the porous liver base on N = 1 and t = 300 s at various microwave power; (a) 8 W (b) 10 W and (c) 12 W

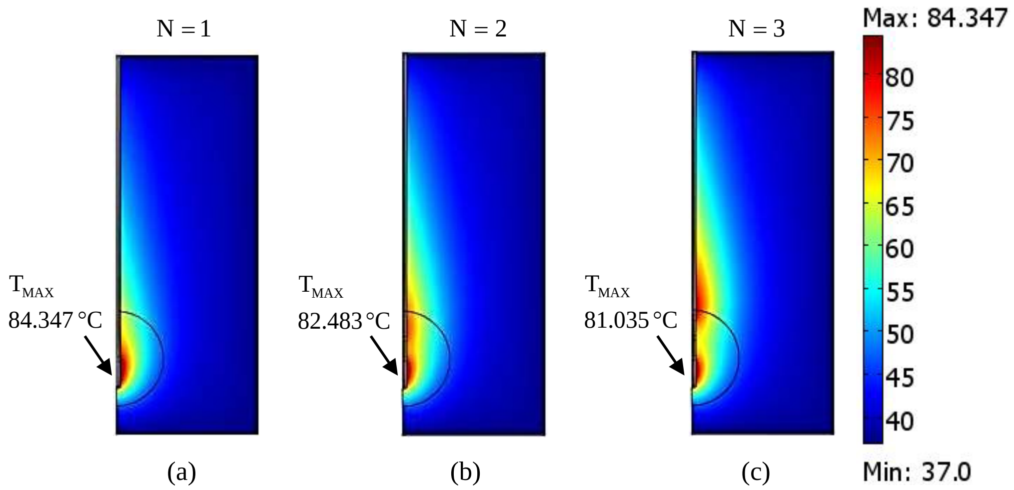

Fig. 9 The temperature pattern within the porous liver base on P = 10 W and t = 300 s at various number of slots; (a) 1 slot (b) 2 slots s and (c) 3 slots

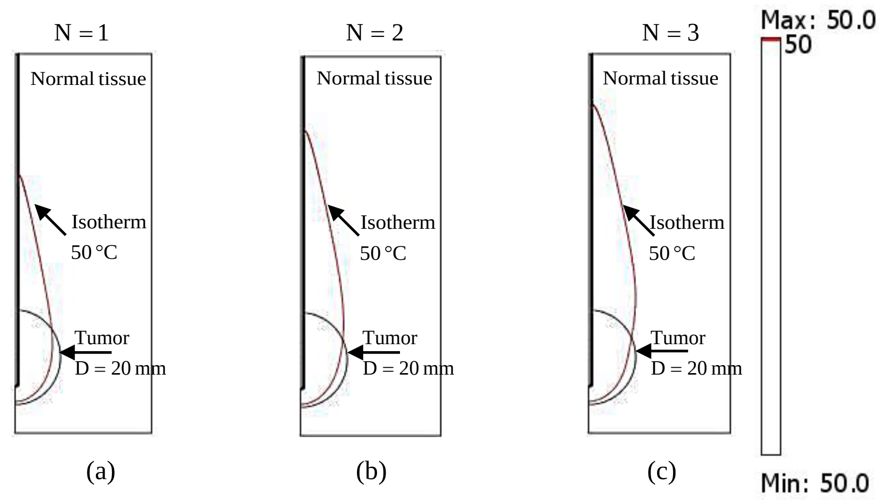

Fig. 10 The ablation area and residual tail length results within the porous liver base on P = 10 W and t = 300 s at various number of slots; (a) 1 slot (b) 2 slots s and (c) 3 slots